Mitochondria as a Platform for Dictating the Cell Fate of Cultured Human Corneal Endothelial Cells

Kohsaku Numa,[1] Morio Ueno,[1] Tomoko Fujita,[1] Koji Ueda,[2] Nao Hiramoto,[1] Atushi Mukai,[1] Yuichi Tokuda,[3] Masakazu Nakano,[3] Chie Sotozono,[1] Shigeru Kinoshita,[4] and Junji Hamuro[1]

[1]Department of Ophthalmology, Kyoto Prefectural University of Medicine, Kyoto, Japan
[2]Project for Personalized Cancer Medicine, Cancer Precision Medicine Center, Japanese Foundation for Cancer Research, Tokyo, Japan
[3]Department of Genomic Medical Sciences, Kyoto Prefectural University of Medicine, Kyoto, Japan
[4]Department of Frontier Medical Science and Technology for Ophthalmology, Kyoto Prefectural University of Medicine, Kyoto, Japan

Correspondence: Junji Hamuro, Department of Ophthalmology, Kyoto Prefectural University of Medicine, 465 Kajii-cho, Hirokoji-agaru, Kawaramachi-dori, Kamigyo-ku, Kyoto 602-0841, Japan; jshimo@koto.kpu-m.ac.jp.

Received: August 21, 2020
Accepted: November 3, 2020
Published: December 4, 2020

Citation: Numa K, Ueno M, Fujita T, et al. Mitochondria as a platform for dictating the cell fate of cultured human corneal endothelial cells. *Invest Ophthalmol Vis Sci.* 2020;61(14):10. https://doi.org/10.1167/iovs.61.14.10

Purpose. Aiming to clarify the role of mitochondria in cell fate decision of cultured human corneal endothelial cell (cHCEC) subpopulations.

Methods. The mitochondrial respiratory ability were examined with Mito stress and Mito fuel flex test assays using an extracellular flux analyzer (XFe24; Agilent Technologies; Santa Clara, CA) for human corneal endothelium tissues, mature cHCECs and a variety of cell state transitioned cHCECs. Tricarboxylic acid cycle and acetyl-coenzyme A–related enzymes was analyzed by proteomics for cell lysates using liquid chromatography–tandem mass spectrometry for cHCEC subpopulations.

Results. The maximum oxygen consumption rate was found to become stable depending on the maturation of cHCECs. In the Mito stress tests, culture supplements, epidermal growth factor, SB203580, and SB431543 significantly repressed oxygen consumption rate, whereas a Rho-associated protein kinase inhibitor Y-27632 increased. Tricarboxylic acid cycle and mitochondria acetyl-coenzyme A–related enzymes were selectively upregulated in mature cHCECs, but not in cell state transitioned cHCECs. The maximum oxygen consumption rate was found to be higher in healthy human corneal endothelium tissues than those with deeply reduced cell density. An upregulated tricarboxylic acid cycle was linked with metabolic rewiring converting cHCECs to acquire the mitochondria-dependent oxidative phenotype.

Conclusions. Mitochondrial metabolic intermediates and energy metabolism are tightly linked to the endothelial cell fate and function. These findings will help us to standardize a protocol for endothelial cell injection.

Keywords: cultured corneal endothelial cell, mitochondria, TCA cycle, acetyl-CoA, flux analyzer, human tissue

As a new frontier of regenerative medicine, cell therapy is progressively being updated to become a new alternative treatment for many noncurable diseases. Human corneal endothelial (HCE) failure with loss of CE cells (CECs) is associated to pathological conditions, such as Fuchs' endothelial corneal dystrophy.[1] We have developed a novel, clinically effective therapeutic modality to regenerate CE tissues by injection of cultured human CECs (cHCECs).[2–9] This novel therapy leads patients to a stable recovery of the transparency and thickness of the cornea and, hence, visual acuity.

How CECs are able to generate and use metabolic energy from the environmental substrates is a critical issue to understand the pathogenesis underlying the CE dysfunctions. The capacity of HCECs for mitochondrial oxidative phosphorylation (OXPHOS) and glycolysis is likely to provide significant insight into the influence of cellular energy status on endothelial pump function, including Na^+K^+-dependent ATPase.[10–14] Mitochondrial OXPHOS and glycolysis are the most relevant metabolic pathways for producing adenosine triphosphate (ATP), which is indispensable to HCEC function.[14,15] The major function of mitochondria in cellular homeostasis has historically been the generation of ATP through OXPHOS.[15–19] Therefore, clarification of the role of mitochondrial OXPHOS and glycolysis in HCE tissue homeostasis is likely to provide significant insight into the influence of cellular energy status on physiologic endothelial cellular integrity.

In a previous study, we found a way to discriminate subpopulations (SPs) in cHCECs by their secretory metabolites, directly or indirectly related with mitochondrial OXPHOS and glycolysis,[9,20] such as lactate and pyruvate, and we found that the cell state transitioned (CST) SPs exhibited a disposition for anaerobic glycolysis instead of mitochondria dependent OXPHOS.[9,20] To the best of our knowledge, these findings are the first to open a way

Copyright 2020 The Authors

This work is licensed under a Creative Commons Attribution-NonCommercial-NoDerivatives 4.0 International License.

for monitoring the disposition of cHCECs in regard to their bioenergetics. To evaluate the culture conditions, the proportion (E-ratio) of effector cells designated by cluster of differentiation (CD) markers was assigned by flow cytometry.[7,8] The E-ratio means the percent proportion of effector cells, that is, the well-differentiated cells. The cultures varied in their content of cHCEC SPs classified by the expression profile of CD markers. The SPs of cHCECs with cell surface marker combination of $CD44^{-/+}CD166^{+}$ $CD133^{-}CD105^{-}CD24^{-}CD26^{-}$ (abbreviated, in this text, as $CD44^{-/+}$) had been assigned as effector cells. Therefore, all SPs of cHCECs devoid of this combination profile of CD markers were defined as CST-cHCECs. E-ratios means the proportion of this effector cells; therefore, E-ratios do not definitely separate "effector cells" from "CST cells." For the effective outcome of cell therapy we are considering that the ratio of effector cells, namely the E-ratio, is better to exceed 90%.

Here, a novel, noncontact method for measuring mitochondrial OXPHOS and glycolysis in in vitro cells and HCE tissues using an extracellular flux analyzer (XFe24; Agilent Technologies; Santa Clara, CA) is described.[21–25] This technology has recently been applied to the study of HCECs or HCE tissues by Greiner et al.[15,26] To confirm the decrease in glycolysis and the disposition for mitochondria-dependent OXPHOS in the mature differentiated cHCECs, we investigated the oxygen consumption rate (OCR) of the diverse cHCEC SPs and HCE tissues. It was suggested that the analysis of cellular oxygen consumption is a new tool to functionally distinguish these cHCEC SPs.

In addition, a proteome analysis of the pathways for the tricarboxylic acid (TCA) cycle and pyruvate metabolism revealed that isozymes responsible for these metabolic pathways in mitochondria were upregulated selectively in mature cHCECs, whereas those in cytosol-nucleus were in the CST-cHCECs.

Methods

Human Corneal Tissue and Endothelial Cell Donors

The human tissue used in this study was handled in accordance with the tenets set forth in the Declaration of Helsinki. HCECs were obtained from human donor corneas via the CorneaGen Inc. (Seattle, WA) eye bank and cultured before the experimental analysis. Informed written consent for eye donation for research was obtained from the next of kin of all deceased donors. All tissues were recovered under the tenets of the Uniform Anatomical Gift Act of the state in which the donor's consent was obtained and the tissue was recovered. All donor corneas were handled as described (Supplementary Table S1).[7–9]

Reagents

The rho-associated protein kinase inhibitor Y-27632 (Y) to promote the cell differentiation and epidermal growth factor (EGF) originally used to promote the cell proliferation[5,7] were purchased from Wako Pure Chemical Industries, Ltd. (Osaka, Japan), and a p38 MAP kinase inhibitor SB203580 (SB2) from Cayman Chemical (Ann Arbor, MI) was used to block the cell senescence. SB431543 (SB4), originally thought to block the negative effect of transforming growth factor-β on cultures,[5,7] Dulbecco's modified Eagle's medium–high glucose and fetal bovine serum were obtained from Gibco Industries Inc. (Langley, OK), and plastic culture plates were obtained from Corning (Corning, Inc., Corning, NY). Oligomycin, carbonyl cyanide 4-(trifluoromethoxy) phenyl-hydrazone (FCCP), rotenone and antimycin, UK5099, Bis-2-(5-phenylacetamido-1.3.4-thiadiazol-2-yl) ethyl sulfide (BPTES), and etomoxir were purchased from Agilent Technologies.

Cell Cultures and Fluorescence Activated Cell Sorter Analysis of cHCECs

Our group have been exploring (for almost 10 years with more than 2000 HCEC cultures) the best and most practical process to provide cHCECs suitable for cell injection therapy as a new modality in place of corneal transplantation. Therefore, the effects of culture supplements, so far tried, on mitochondrial respiratory ability were examined (EGF, SB4, SB2, and Y-27632). The HCECs were cultured according to the published protocols, with some modifications.[5] Briefly, the Descemet's membranes with the CECs were stripped from donor corneas and digested at 37°C with 1 mg/mL of collagenase A (Roche Applied Science, Penzberg, Germany) for 2 hours. The HCECs obtained from a single donor cornea were seeded in one well of a type I collagen-coated six-well plate (Corning, Inc., Corning, NY). The culture medium was prepared according to published protocols.[9,20] HCECs at passages two to four were used for all experiments. Phase-contrast images were obtained using an inverted microscope system (CKX41; Olympus Corporation, Tokyo, Japan). HCECs were collected for fluorescence activated cell sorter analysis according to the procedures described previously.[7,8] The labeled cHCECs were analyzed using a BD fluorescence activated cell sorter Canto II (BD Biosciences, San Jose, CA) fluidics-system flow cytometer.

Analysis of Platelet-Derived Growth Factor (PDGF)-$\beta\beta$ and IL-8 in CSs

Culture supernatants (CSs) were harvested from the cultures of cHCECs and centrifuged at $1580\times g$ at room temperature for 10 minutes to remove detached cells. The CSs were collected and filtered through 0.22-µm filters (Millex-GV; EMD Millipore Corporation, Temecula, CA). An ELISA was performed using a PDGF-$\beta\beta$ and interleukin 8 (IL-8) Human ELISA Kit (Abcam Plc., Cambridge, UK), as described.[9]

Cell and Human Corneal Endothelium Tissue Preparation for Flux Analysis

Cells were seeded in XF24 cell culture plates (40,000 cells per well; the cell density screened and predetermined optimum) and incubated overnight at 37°C in 5% CO_2. The preparation of HCE tissues was performed following Greiner et al.'s protocols.[15] One day before analysis, the endothelium–Descemet membrane complex was prestripped using a standardized technique for Descemet membrane endothelial keratoplasty graft preparation with minor modifications. On the day of the assay, prestripped corneas were warmed to 25°C for 1 hour, then mounted on a vacuum trephine. Under Optisol GS (Chiron Vision, Irvine, CA), partial thickness punches through the endothelium–Descemet membrane complex were made using a biopsy punch of 3 mm in diameter (Integra Life Sciences, Plainsboro, NJ). Each tissue punch was secured endothelium side up on a 4-mm diameter punch of transparent backing

Investigative Ophthalmology & Visual Science

membrane (Millicell Cell Culture Inserts, 1.0 µm polyethylene terephthalate; EMD Millipore, Billerica, MA) using a 1:2 mixture of Matrigel extracellular matrix (Corning Incorporated, Tewksbury, MA) diluted in XF Base Media (Agilent Technologies). The coupled tissue and backing were placed in the bottom of an XFe24 cell culture microplate (Agilent Technologies) and submerged in Optisol GS. Tissue mounts were rinsed and maintained in assay medium for 1 hour at 37°C before assay. For all experiments, experimental groups consisted of at least three biological replicates and technical duplicates were used. Data shown are representative for multiple independent experiments.

Real-Time Metabolic Analyses

Real-time metabolic analysis of live cHCECs and HCE tissue was performed using the Seahorse XFe24 extracellular flux analyzer (Agilent Technologies). HCECs from a healthy young donor (14 years of age) were cultured in Nancy medium until passage 2, and these cells were seeded to a XF24 flux analyzer plate. The wells were divided into two groups, supplemented with or without 0.5 ng/mL EGF and cultured for a further 24 hour (cHCECs #223-2) or supplemented with or without 1 µM SB431542, and cultured further for 72 hour (cHCECs #222). EGF or SB4 were added 24 or 72 hours before the Mito stress test, respectively, because they are functioning in these short exposure periods to cHCECs. In addition, HCECs obtained from a healthy young donor (29 years of age) were cultured and seeded to a XF24 flux analyzer plate similarly. After 11 days of culture in the presence of Y-27632, the cells were divided into two subgroups and cultured with or without Y-27632. A Mito stress test was performed on day 14. Because Y-27632 is used throughout the culture period because of its multiple biological effects working for a long period, the cultures were continued for the initial 10 days with or without Y-27632, and the two groups were further divided into four groups, the final addition and nonaddition, 72 hours before the Mito Stress test. The different timelines for the different supplements were based on our consideration on the kinetics of the action exerted by these supplements.

For the Mito Stress and Fuel Dependency tests, cell culture medium or Optisol GS was replaced 1 hour before the assay with minimal XF Dulbecco's modified Eagle's medium supplemented with 2 mM/L glutamine, 10 mM/L glucose, and 1 mM/L sodium pyruvate (pH 7.4). The OCR and the extracellular acidification rate (ECAR) was analyzed at basal conditions and after sequential injections of 1 µM oligomycin, 1 µM FCCP, 0.5 µM rotenone, and antimycin A.

Tissue Mito Stress Assay Post-Processing

Following metabolic assays, tissue punches were fixed for 20 minutes using 4% paraformaldehyde in PBS, rinsed with Tris-buffered saline, and labeled fluorescently for 20 minutes using 1:1000 Hoechst 33342 (Dojindo Laboratories, Kumamoto, Japan) diluted in PBS. Tissues were rinsed and maintained in PBS for imaging on a fluorescence microscope (BZ-9000, Keyence, Osaka, Japan). Images were captured using a 4× objective with a 200-ms exposure and a FITC filter; multiple images were taken to cover the entire punch area. Montaged images were imported into ImageJ,[28] the threshold function was used to generate binary images labeling only the nuclei, and the particle analysis function was used to count the number of individual nuclei (cells). Cell counts were used to normalize the metabolic assay results to generate ECAR/cell and OCR/cell values.

Mito Fuel Flex Dependency Test Assays

For the analysis of mitochondrial fuel oxidation pathway, a Mito Fuel Dependency test (Agilent Technologies) was performed according to the manufacturer's instructions at recommended drug concentrations Table. Briefly, the Mito fuel flex test inhibits the importation of three major metabolic substrates (pyruvate, fatty acids, and/or glutamine) with mitochondrial pyruvate carrier inhibitor UK5099 (2 mM), carnitine palmitoyltransferase 1A inhibitor etomoxir (4 mM), or glutaminase inhibitor BPTES (3 mM). Baseline OCR was monitored for 18 minutes followed by sequential inhibitor injections (i.e., Treatment 1 or Treatment 2) with OCR readings for 1 hour after each treatment. Four lots of cHCECs (#a53, #1010, #a34, and #231s) were used in this analysis.

Proteomics by Liquid Chromatography-Tandem Mass Spectrometry (LC/MS)

To gain the insight on the mitochondrial OXPHOS activity among cHCEC SPs, proteomics by LC/MS were performed. The cell lysates of cHCECs at passage four were used. The proteome analysis for 4641 proteins in total were performed, as recently described in detail.[9,27] The analysis for the enzymes involved in the TCA cycle and pyruvate metabolism is firstly presented here. The high-quality cHCECs containing the $CD44^{-/+}$ mature differentiated cHCEC SPs at a ratio of 93.9% (effector ratio = E-ratio, $n = 3$) and the low-quality cHCECs containing the CST-$CD44^{++/+++}$ immature cHCEC SPs at a ratio of 73.8% ($n = 3$) were analyzed. The procedures for the preparation of these two SPs and the proteome analysis were recently detailed (Supplementary Fig. S1).[9,27] Lysates from three aliquots of each high-quality or low-quality cHCEC were provided for the analysis. Peptides were analyzed using an LTQ-Orbitrap-Velos mass spectrometer (Thermo Fisher Scientific, Inc., Waltham, MA) combined with an Ulti-Mate 3000 RSLC nano-flow HPLC system (Thermo Fisher Scientific, Inc.). Protein identification and quantification analysis were performed with MaxQuant software. The MS/MS spectra were searched against the *Homo sapiens* protein database in Swiss-Prot, with a false discovery rate set to 1% for both peptide and protein identification filters. Only "Razor1unique peptides" were used for the calculation of relative protein concentration. The LC/MS data set, composed of 4641 proteins in total, was obtained by use of Proteome Discoverer 2.2 software. After removal of the data in which the abundance ratio could not be calculated, we analyzed the remaining data by means of a web-based program, DAVID v6.8 (The Database for Annotation, Visualization and Integrated Discovery; https: //david.ncifcrf.gov). Finally, it ended up with 4315 genes, each with a unique DAVID Gene ID, for the subsequent analyses. Further investigations for the focused genes were performed by using DAVID and its options "BIOCARTA" and "KEGG_PATHWAY." We referred their original databases of BioCarta (https: //cgap.nci.nih.gov/Pathways/BioCarta_Pathways) or KEGG (Kyoto Encyclopedia of Genes and Genomes; https://www.genome.jp/kegg/) and showed the referred genes/pathways in the figures with slight modifications. For the clarity of the procedures, the details of the procedures were cited here from the reference 5 as Supplementary Fig. S2, together with the detailed legend.

Investigative Ophthalmology & Visual Science

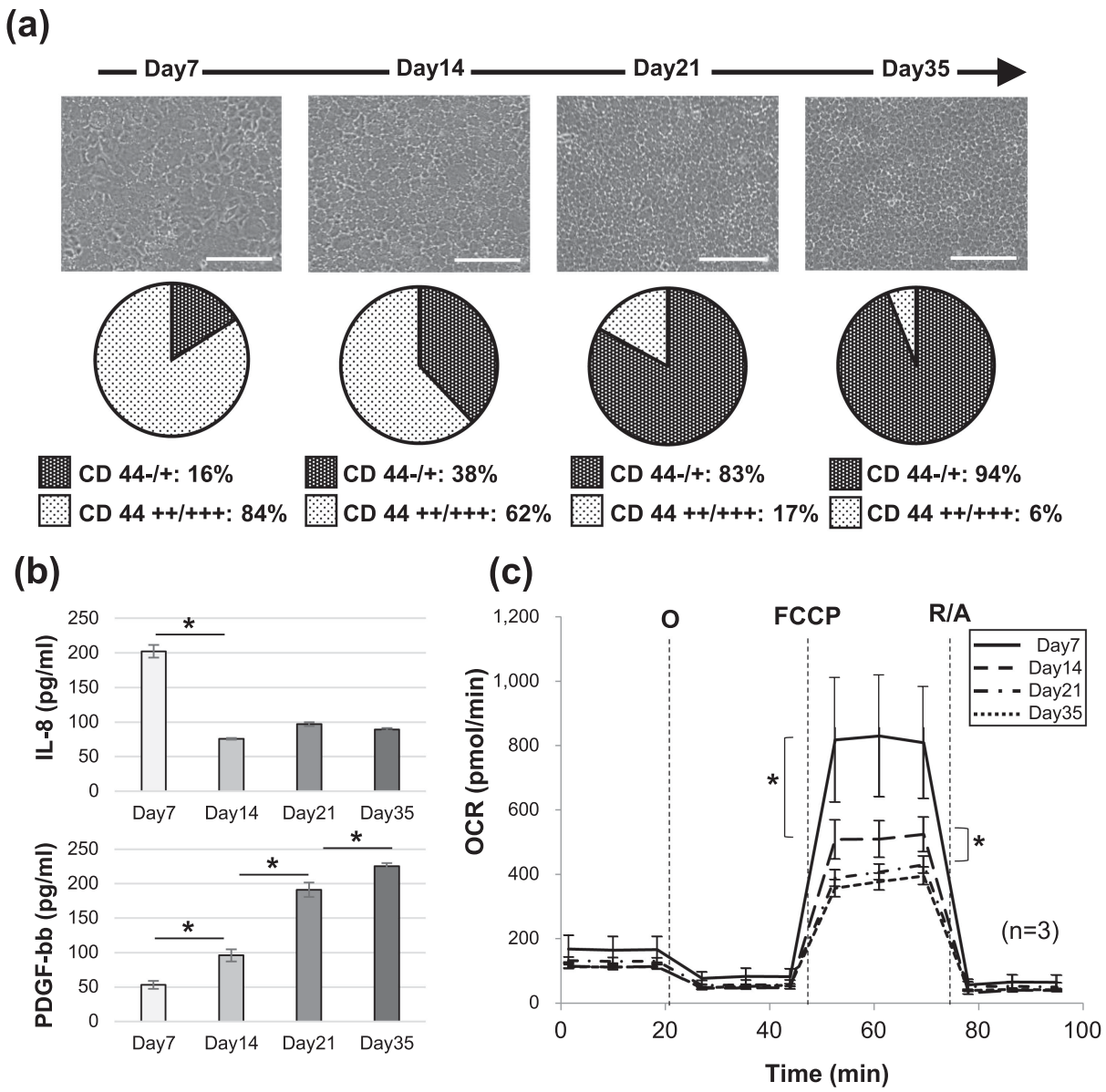

Figure 1. Changes in the maximum OCR during the maturation process of cHCECs. Cells at 7, 14, 21, and 35 days after passage were examined. **(a)** Change of cellular morphology (scale bar = 100 µm) and the proportions of cHCEC SPs visualized by a fluorescence activated cell sorter (FACS) (CD44). **(b)** Changes in secreted IL-8 and PDGF-$\beta\beta$ in the CSs measured by ELISA. **(c)** Change in mitochondrial respiration in the mature SPs determined by the Mito stress test assay. (*$P < 0.05$) Dashed lines in **(C)** indicate the assay drug injections and abbreviations above them represent specific compounds injected. Oligomycin inhibits ATP synthase (complex V). It decreases electron flow through the electron transport chain (ETC), resulting a reduction in mitochondrial respiration or OCR. This decrease in OCR is linked to cellular ATP production. Carbonyl cyanide-4 (trifluoromethoxy) phenylhydrazone (FCCP) is an uncoupling agent that collapses the proton gradient. As a result, electron flow through the ETC is uninhibited, and oxygen consumption by complex IV reaches the maximum. The FCCP-stimulated OCR can then be used to calculate spare respiratory capacity, defined as the difference between maximal respiration and basal respiration. Spare respiratory capacity is a measure of the ability of the cell to respond to increased energy demand or under stress (for example, *in vivo* pumping action of corneal endothelial cells). The third injection is a mixture of rotenone, a complex I inhibitor, and antimycin A, a complex III inhibitor. This combination shuts down mitochondrial respiration and enables the calculation of nonmitochondrial respiration driven by processes outside the mitochondria. The details were also indicated in reference. FCCP, carbonyl cyanide-p-trifluoromethoxyphenylhydrazone; O, oligomycin; R/A; Rotenon/Antimycin A.

Investigative Ophthalmology & Visual Science

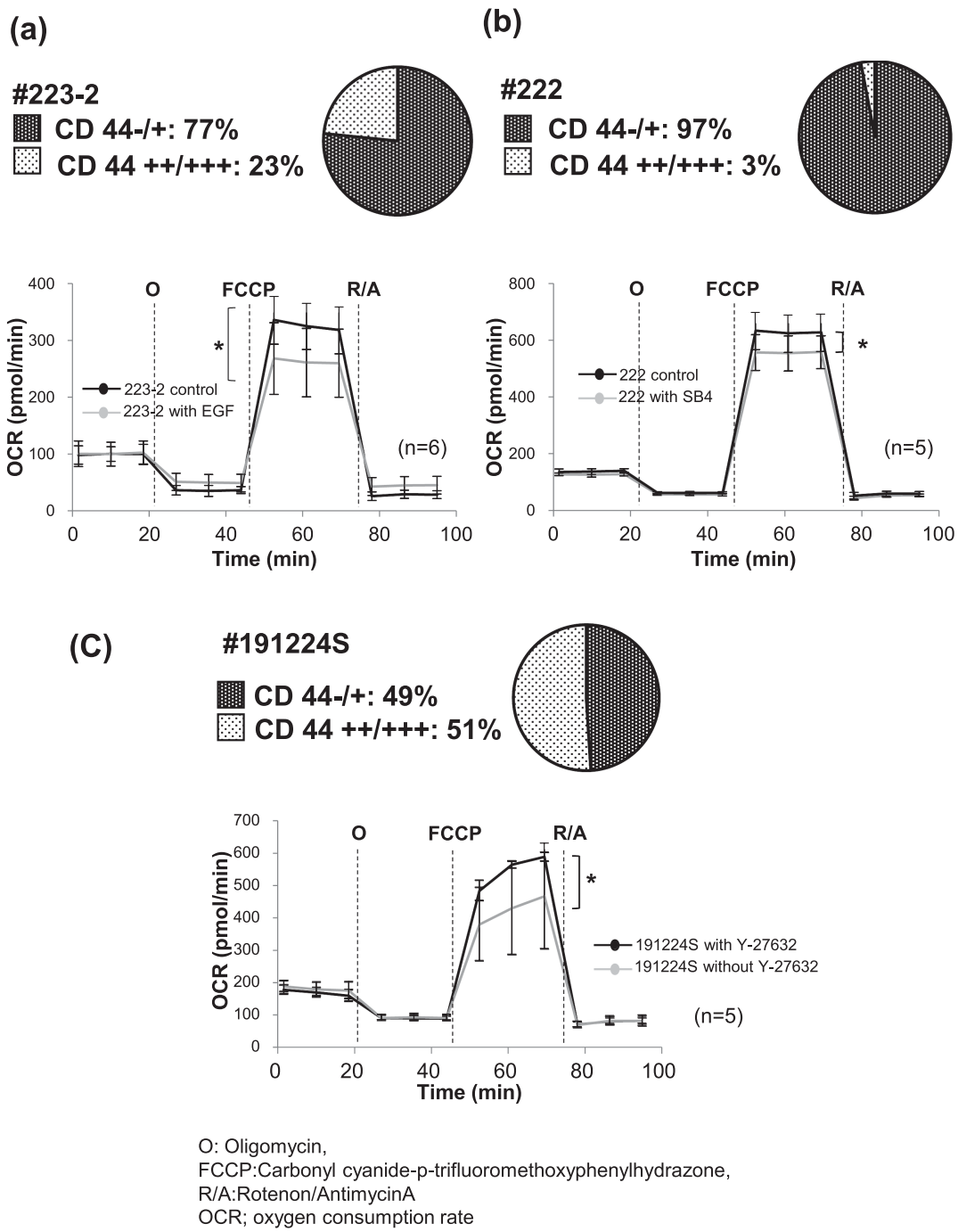

Figure 2. Change of mitochondrial function OXPHOS in cultures supplemented with EGF, SB203580, SB431542, or Y-27632. **(a)** Human cHCECs from a healthy young (14 years) donor #223-2 were cultured in Nancy medium until passage 2, There was a significant difference in the maximum OCR between cHCECs with EGF and control (*$P < 0.05$). **(b)** HCECs (#222) from a healthy young (14 years) donor were cultured in Nancy medium until passage 2, There was a significant difference in the maximum OCR between cHCECs with and without SB4 (*$P < 0.05$). **(c)** HCECs obtained from a healthy young (29 years) donor #191224S were cultured in Nancy medium until passage 2, There was a significant difference in the maximum OCR between #191224S(Y+/+) and (Y+/−) (*$P < 0.05$). All the experimental groups consisted of at least three biological replicates. Dashed lines in **(a)**, **(b)**, and **(c)** indicate the assay drug injections and abbreviations above them represent specific drugs injected. FCCP, carbonyl cyanide-p-trifluoromethoxyphenylhydrazone; O, oligomycin; R/A, Rotenon/Antimycin A.

Investigative Ophthalmology & Visual Science

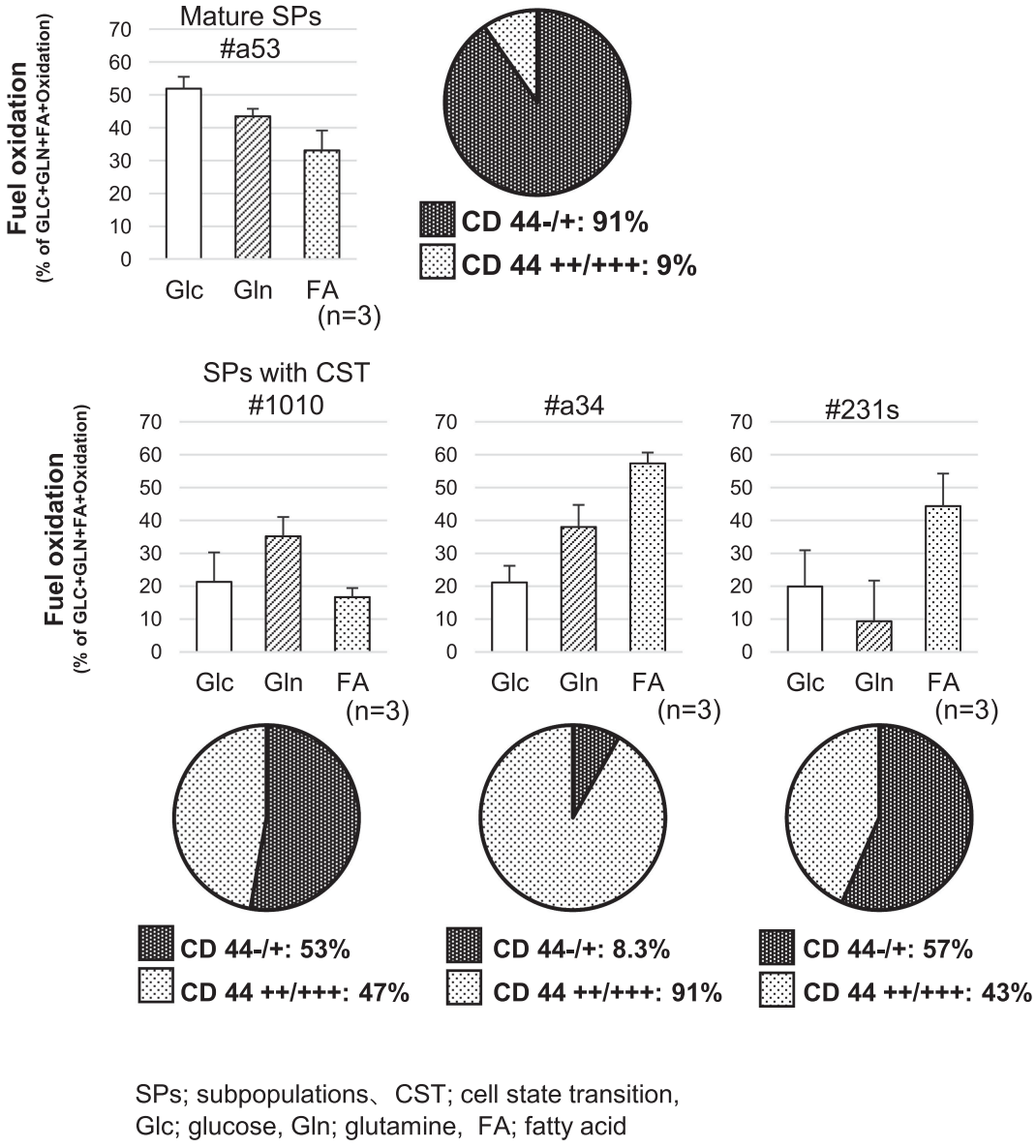

Figure 3. Fuel dependency of cultured HCECs to oxidize glucose (pyruvate), glutamine (glutamate), and fatty acids of mitochondrial respiration. Each dependency was measured by the treatment of inhibitors, including UK5099, Bis-2-(5-phenylacetamido-1.3.4-thiadiazol-2-yl) ethyl sulfide (BPTS), and etomoxir. Five different lots of mature cHCECs and 11 different lots of CST cHCECs were investigated in 4 replicates and the figures shows the representative results, one for the former and three for the latter.

Statistical Analysis

Data were analyzed using EZR (Saitama Medical Center, Jichi Medical University, Saitama, Japan), which is a graphical user interface for R (The R Foundation for Statistical Computing, Vienna, Austria).[29] More precisely, it is a modified version of R commander designed to add statistical functions frequently used in biostatistics. An unpaired two-tailed Student t test was performed when applicable. Data were considered statistically significant at a P value of less than 0.05.

Results

Changes in Energy Flux during the Maturation of cHCECs

To monitor mitochondrial respiration and glycolysis in in vitro cells, it should be necessary to stage the cHCEC dynamics, either as proliferative, differentiating, or fully matured, because the energy demand will vary depending on these cell dynamics. A Mito stress test was performed using cHCECs at 7, 12, 24, and 35 days after cell passaging. The

Investigative Ophthalmology & Visual Science

E-ratios climbed during the proliferative stage of the culture period and reached 94% by 35 days (Fig. 1a).

IL-8 and PDGF-$\beta\beta$ in CSs had been proven to be the standardized biomarkers in qualifying the differentiation status of the produced cHCECs.[9] IL-8 in CSs, known to decrease during the proliferation period, decreased by day 14, whereas PDGF-$\beta\beta$ in CSs , known to increase during the differentiation and maturation period,[20] increased by day 35 (*$P < 0.05$, Fig. 1b). It is noteworthy that OCR well paralleled the kinetic change of PDGF-$\beta\beta$ and the increase of E-ratios (Fig. 1c), implying that the energy demand of cHCECs become stable after the differentiation and maturation of cHCECs. No difference was observed in the baseline OCR, but the maximum OCR was significantly higher on days 7 and 14 than on days 21 and 35 (*$P < 0.05$) and stabilized as differentiation and maturation proceeded by day 35 (Supplementary Fig. S3).

Diverse Changes of OXPHOS by Culture Supplements

In the course of establishing the newly improved protocol of manufacturing cHCECs, the following were confirmed in regards to the supplements used here and published.[8] The continuous presence of Rho-associated protein kinase inhibitor Y-27632 greatly increased the E-ratios, whereas the presence of transforming growth factor-β/Smad-inhibitor SB4 greatly decreased the E-ratios and number of recovered cHCECs.[8] The seeding cell density during culture passages proved vital for maintaining high E-ratios for the extended passages.[8] SB2 did not affect the E-ratios, but EGF caused a significant reduction, even at a concentration of 1 µg/mL.[8]

In the Mito stress tests, it turned out that the addition of EGF (Fig. 2a) and SB4 (Fig. 2b) showed a significant decrease (*$P < 0.05$) in the maximum OCR. The deletion of Y-27632 decreased the maximum OCR (Fig. 2c), and the effect of the deletion of Y-27632 appeared at 72 hours after treatment.

Diversity of Metabolic Substrate Dependency

We examined the substrate specificity of respiration in cHCEC SPs shown in Figure 3, that is, the metabolism dependence of the three major substrates—glucose, amino acids, and fatty acids. It was found that various profiles were exhibited. As previously described,[7–9,20] CST-cHCEC SPs were highly heterogeneous compared with strictly qualified mature cHCECs regarding the surface CD antigen expression profiles, such as CD44, CD24, and CD90. Therefore, it is difficult to deduce a simple summary for the cardinal features in metabolic substrate dependency for CST-cHCEC SPs (more than 11 different lots of CST-cHCECs were investigated). However, representative mature SPs exhibited the tendency to be glucose dependent more than CST-SPs and, instead, CST-SPs showed the tendency more dependent on glutamine and fatty acid as substrates, and thus, more anaplerotic (Fig. 3). The further precise and extended works are the prerequisite for the definitive conclusion.

Assessment of OXPHOS Activity in Endothelium Tissues

To gain the standardized procedures to quantify the average OCR/cells and ECAR/cells among the CE tissues, average OCR/cells, ECAR/cells, and estimates of variability were

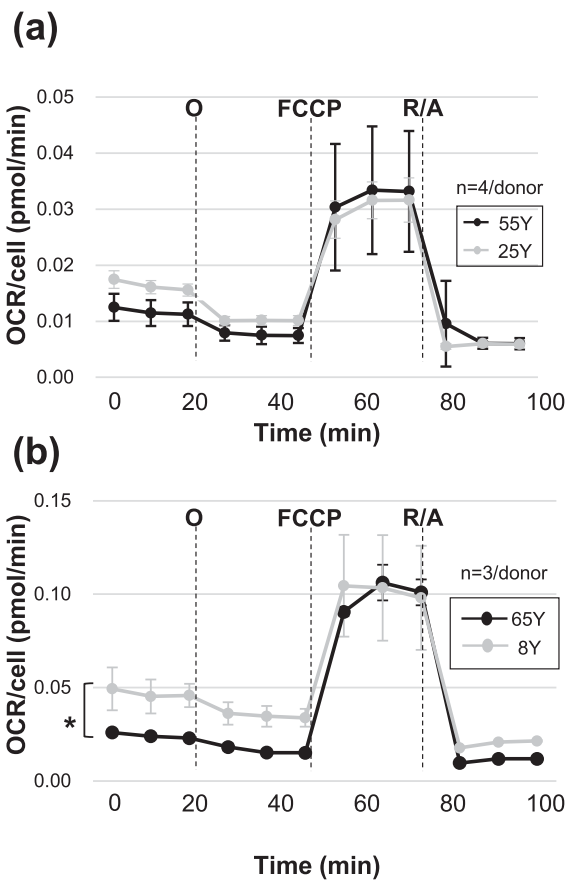

O: Oligomycin,
FCCP:Carbonyl cyanide-p-trifluoromethoxyphenylhydrazone,
R/A:Rotenon/AntimycinA

OCR; oxygen consumption rate, Y; year old

Figure 4. Direct analysis of energy-producing metabolic activity in the corneal endothelial (CE) tissues. Comparison of mitochondrial respiration among distinct CE tissues. **(a)** The first was the comparison of the tissues from a 25-year-old male (punched tissues contained 18,139 ± 1138 cells [average ± SD] by cell counting with Hoechst staining after Mito stress test assay) and a 55-year-old woman (punched tissues; 18,139 ± 1138 cells [average ± SD]) (n = 4/donor). **(b)** The second was those between an 8-year-old boy (punched tissues; 9627 ± 673 cells) and a 65-year-old man (punched tissues; 12,455 ± 1311 cells) (n = 3 per donor). Experimental groups consisted of four technical duplicates. Dashed lines indicate the assay drug injections and abbreviations above them represent specific drugs injected. FCCP, carbonyl cyanide-p-trifluoromethoxyphenylhydrazone; O, oligomycin; R/A, Rotenon/Antimycin A.

investigated firstly among the HCE tissues of 12 different donors (a total of 48 times repetition of different HCE tissue pieces). The baseline OCR were slightly distinct among the donors, but no difference was found in the maximum OCR among the HCE tissues of donors different in their ages between 6 and 70 years (representative results are illustrated in Figs. 4a, b). Next, we compared a 53-year-old healthy CE and the 43-year-old CE with an endothelial cell density of 400 cells/mm^2 with guttae (repeated eight times to gain accurate averages). The maximum OCR, reflecting the in vivo ATP-producing activity, was found to be significantly higher in normal CE than it was in CEC decompensation (Fig. 5).

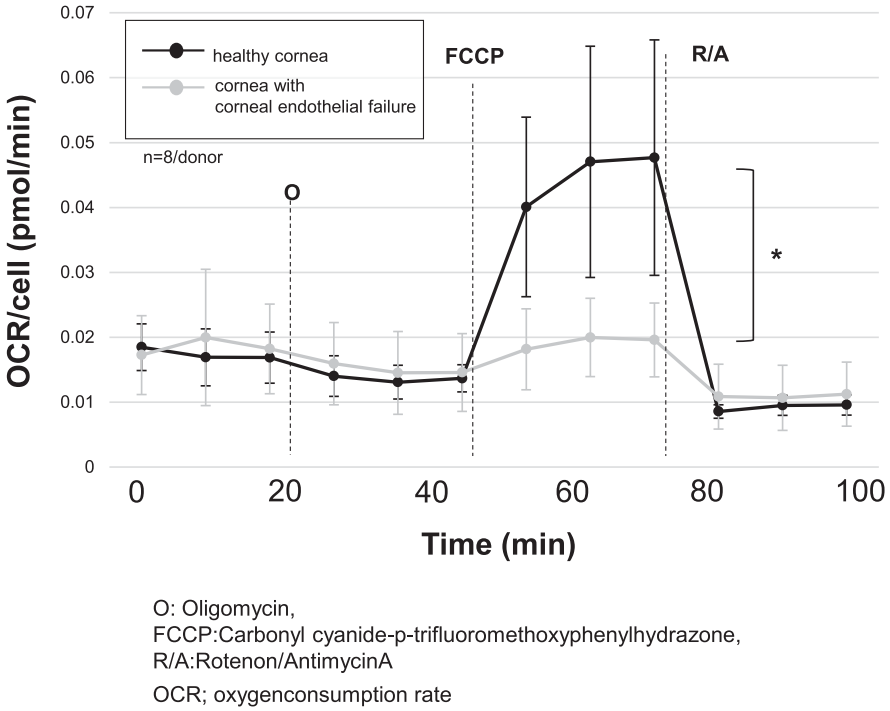

Figure 5. Direct analysis of energy-producing metabolic activity in the corneal endothelial (CE) tissues. Comparison of mitochondrial respiration between CE tissues from healthy cornea and those from cornea with CE decompensation ($n = 8$ per donor). The detailed donor information was as follows; healthy corneas were from 55 year old male donor, and the endothelial cell density (ECD) of the right and left eye were 2519 and 3021 cells/mm^2, respectively (punched tissues contained 12,821 ± 1935 cells [average ± SD]), by cell counting with Hoechst staining after Mito stress test assay). Corneas with endothelial failure were from a 43-year-old woman and the ECD values of the right and left eyes were 654 and 142 cells/mm^2, respectively (punched tissues; 7531 ± 1966 cells). Experimental groups consisted of four technical duplicates. Dashed lines indicate the assay drug injections and abbreviations above them represent specific reagents injected. FCCP, carbonyl cyanide-p-trifluoromethoxyphenylhydrazone; O, oligomycin; R/A, Rotenon/Antimycin A.

TCA Cycle and Pyruvate Metabolism

Investigations of the focused genes and the related pathways involved in cHCEC metabolism were performed. The part of the genes/pathways involved in LC/MS data set and analyzed by means of a web-based program, DAVID v6.8 (Supplementary Fig. S2) is shown for the TCA cycle (Fig. 6a) and the pyruvate metabolism (Fig. 6b). The part of the referred pathways in glycolysis, glutamine, alanine, nicotinamide, and arginine metabolism were presented in our previous publications.[9,27] Differences were found in the expression of enzymes that determine the metabolic pathway of pyruvate; pyruvate carboxylase, and pyruvate dehydrogenase (PDH) upregulated in the mature cHCECs, whereas lactate LDH was upregulated in the CST-cHCECs. Enzymes responsible for the TCA cycle, malate dehydrogenase 1 (MDH1), aconitase 1 (ACO1), and isocitrate dehydrogenase 1 (IDH1) were upregulated in the latter, whereas malate dehydrogenase 2, ACO2, and isocitrate dehydrogenase 2 were upregulated selectively in the former. Expression of enzymes related to acetyl-coenzyme A (CoA) was also in contrast to this; acetyl-CoA synthase short chain 1 (ACSS1) upregulated selectively in the mature SPs, whereas ATP-citrate lyase (ACLY) and acetyl-CoA synthase short chain 2 (ACSS2) upregulated in the CST-SPs.

Distinct Dependence on Pyruvate of Mitochondrial OXPHOS

Considering the implication obtained above on the distinctive pyruvate metabolism between two mature- and CST-cHCEC SPs, we performed the Mito stress test for mature SPs (#223-1) and CST SPs (#226). Although a significant divergence was observed in maximum respiration (*P < 0.05), the divergence disappeared when tested in pyruvate-added medium, implying the impaired metabolic production of pyruvate in the CST-SPs. Thus, exogenous pyruvate may compensate for the disorder of enzymes that determine the metabolic pathway of pyruvate in CST-SPs (Fig. 7).

Discussion

In the current study, we found that extracellular flux analysis of oxygen is a new tool to functionally distinguish cHCEC SPs. The first aim of this study was to determine the mitochondrial function as a platform for dictating the cell state of HCECs. The second was to contribute to improving a protocol for the standardized and reproducible cultures of endothelial "effector" cells polarized in mitochondrial OXPHOS, thereby enabling obtainment of the most homogeneous cHCECs suitable for the

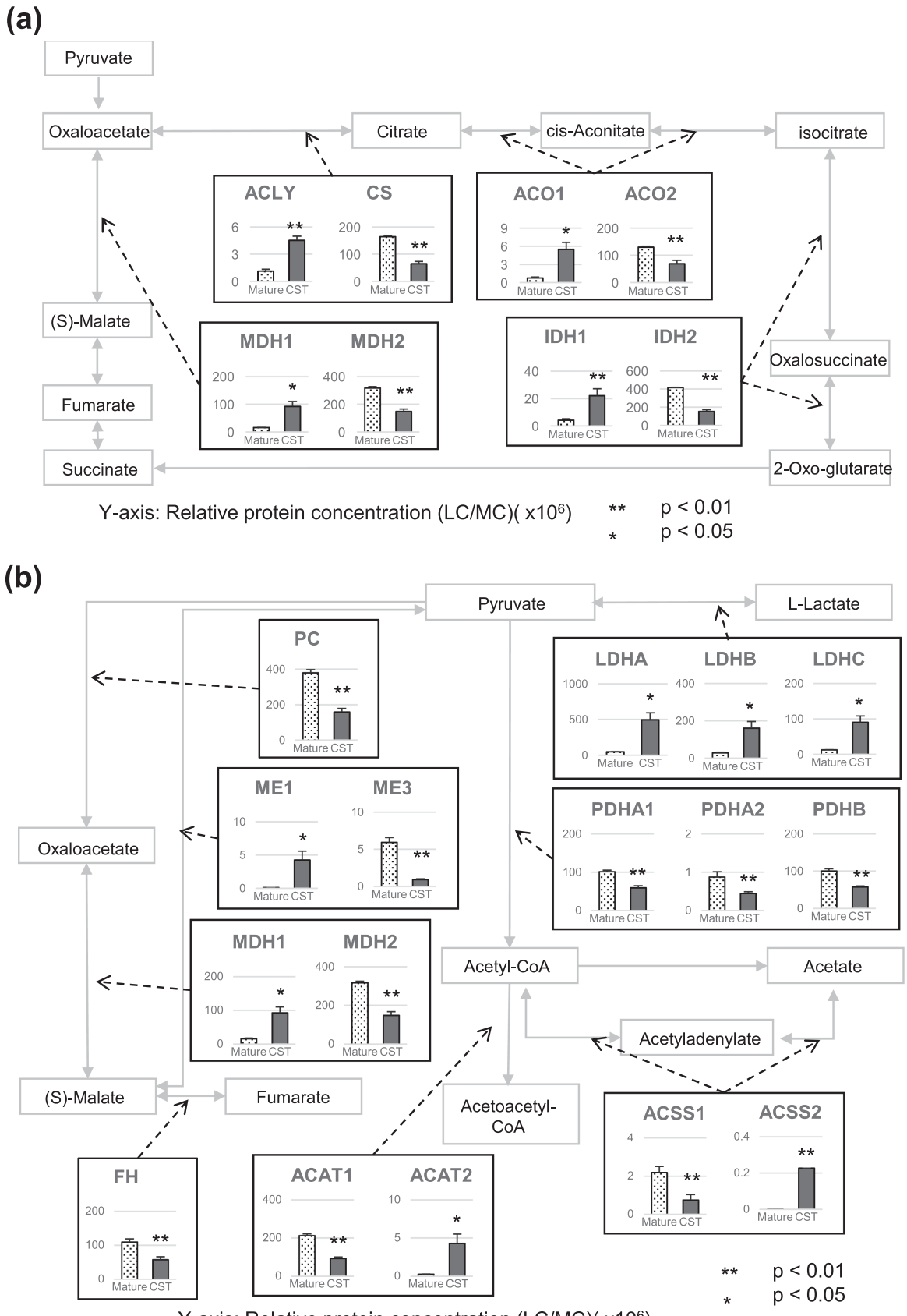

Figure 6. Expression of key enzymes of the TCA cycle and pyruvate metabolism in cultured HCECs (cHCECs). **(a)** TCA cycle. **(b)** Pyruvate metabolism. *$P < 0.05$, **$P < 0.01$. Experimental groups consisted of biological duplicates and technical triplicates.

Investigative Ophthalmology & Visual Science

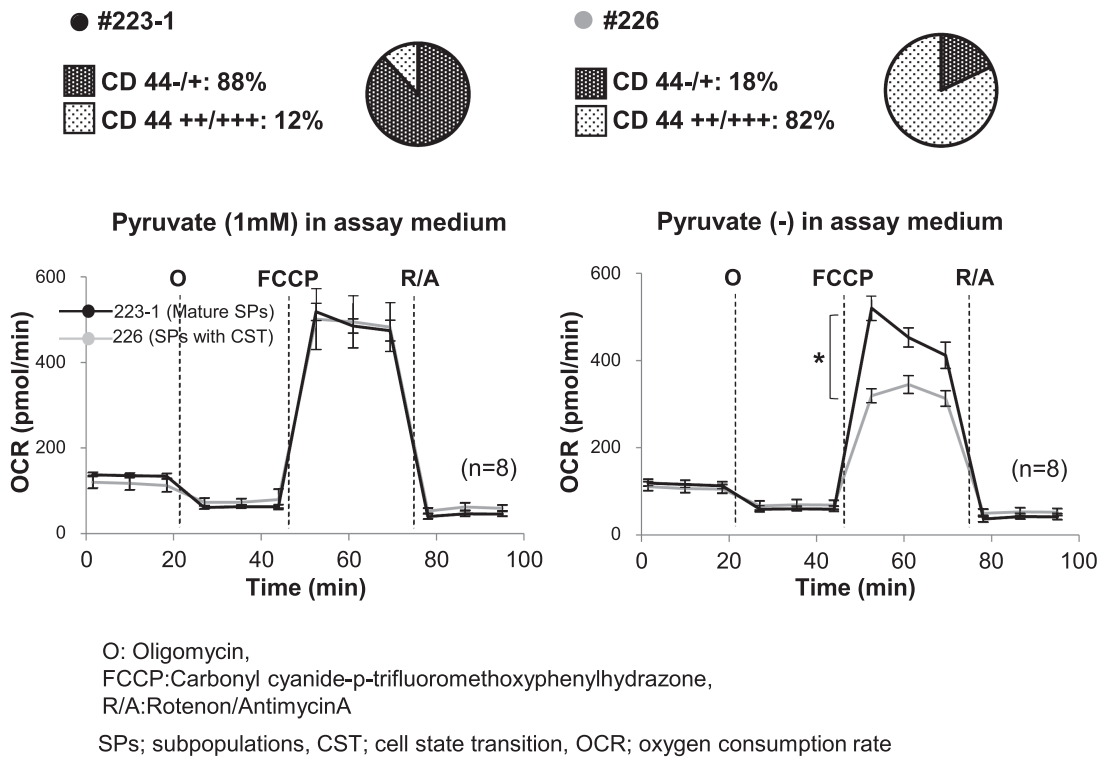

Figure 7. Change of mitochondrial function OXPHOS in cultures supplemented with or without pyruvate. Mito stress tests of #223-1 mature SPs (88% $CD44^{-/+}$ and 12% $CD44^{++/+++}$ cells; black) and #226 CST-SPs (18% $CD44^{-/+}$ and 82% $CD44^{++/+++}$ cells; gray) are illustrated. Maximal respirations decreased in CST SPs in the absence of pyruvic acid. The addition of 1 mM pyruvate in the medium diminished this divergence. There was significant difference in the maximum OCR between #223-1 and 226 when using pyruvate (−) assay medium (*$P < 0.05$). Dashed lines indicate the assay drug injections and abbreviations above them represent specific drugs injected. Experimental groups consisted of both biological and technical triplicates. FCCP, carbonyl cyanide-p-trifluoromethoxyphenylhydrazone; O, oligomycin; R/A, Rotenon/Antimycin A.

cHCECs-injection treatment of HCE dysfunctions. To date, the quality of the in vitro culture of cHCECs has been assessed by fluorescence activated cell sorter in terms of the cell surface CD markers of cHCECs present in situ. The SPs with $CD166^{+}CD44^{-/+}CD133^{-}CD105^{-/+}$ $CD24^{-}CD26^{-}$ phenotypes are currently defined as effector cells for cell injection therapy.[2,7,8] However, little is understood about how the expression of surface CD markers is correlated to the in vivo HCE tissues reconstituting functions of injected cHCECs. The function-based, in vitro and ex vivo quality assessment of HCEC tissues and cHCECs remains a challenge. The cornea's ability to maintain proper hydration depends on the activity of the CE, a process dependent on metabolic energy.[10–15] The observation that maximum OCR, reflecting the in vivo ATP-producing activity, significantly higher in normal CE than it was in CEC decompensation (Fig. 5, Supplementary Fig. S3) imply the usefulness, albeit in part, of here described analysis of cellular oxygen consumption to qualify dysfunctional HCE tissues.

The observation mentioned elsewhere in this article supports our proposed notion[9,20] that CST-cHCECs exhibit a disposition for anaerobic glycolysis instead of mitochondria-dependent OXPHOS contrary to $CD44^{-/+}$ effector cells dominant in OXPHOS. The functional OXPHOS dominancy was validated here by a Mito stress test using Seahorse XF-24 Flux Analyzer (Fig. 1c, Fig. 7). The mitochondrial respiratory function was dynamically varied after the cell seeding, in parallel with the reduced CD44 expression (Figs. 1a, c), until the mitochondrial reserve was stabilized in about 5 weeks. This period was confirmed necessary for the full differentiation of cHCECs indexed, as well as the decreased CD44 expression, by the increased and decreased production of PDGF-$\beta\beta$ and IL-8, respectively[9,30] (Fig. 1b).

The continuous presence of Y-27632 greatly increased the E-ratios, whereas the presence of SB4 greatly decreased the E-ratios.[8] These previous observations correspond quite well with the upregulated OXPHOS in cHCECs produced either in the continuous presence of Y-27632 (Fig. 2c) or absence of SB4 (Fig. 2b). Strikingly, the nonaddition of EGF throughout the culture period reproducibly produced cHCECs polarized in mitochondrial OXPHOS more efficiently than its presence did. Instead, cHCECs produced in the presence of EGF exhibited elevated polarization to glycolysis, even in the continuous presence of Y-27632 (Fig. 2a). Furthermore, in the absence of EGF, mature cHCECs exhibited an elevated OXPHOS inclination in the absence of SB4. To ascertain the reproducible production of homogeneous cHCECs with E-ratios of more than 90%, the continuous presence of Y-27632 and absence of EGF and SB4 throughout the culture period may be preferable. All the results described here are consistent with the long experienced efficacy of gaining cHCECs with high E-ratios either in the presence or absence of these culture supplements, indicating the usefulness of the Mito stress test.

Anaplerosis via glutaminolysis or pyruvate carboxylation contribute to the additional supplies of biosynthetic

precursors not met by glucose metabolism.[31–33] Glutamine is converted to α-ketoglutarate for catabolism through the TCA cycle to malate, which is transported into the cytoplasm and converted to pyruvate and then to lactate.[32] A recent report described that glutaminolysis mainly sustains ATP production in terminally differentiated nonproliferating HCE and accelerates the CE pump function,[31] although the authors described that the relative contribution of glucose and glutamine to the TCA cycle requires further investigation. In accordance with this argument, in our study, the substrate dependency (glucose, glutamine, or fatty acids) of mitochondrial respiration varied largely depending on the differences in the composition of cHCEC SPs (Fig. 3).

Cultured HCECs have an inclination to enter dedifferentiation states, including endothelial mesenchymal transition. Endothelial mesenchymal transition is a dedifferentiation program that rewires the metabolic program to accommodate cellular changes.[34] Among CST-cHCECs, dedifferentiated cHCEC SPs switched to a glycolytic metabotype, eliciting an elevated amount lactate secretion.[9] The catabolic and anabolic pathways in the TCA cycle, operating in the mitochondrial matrix, consist of multiple enzymes, citrate synthase, ACO2, isocitrate dehydrogenase 2, fumarate hydratase, malic acid enzyme 2, and malate dehydrogenase 2. Here, the listed isozymes, all oriented in the mitochondria, were all detected in mature $CD44^{-/+}$ cHCEC SPs (Figs. 6a, b). The induction of acetyl-CoA in cytosol or in the nucleus is supported by the other subsets of counterpart isozymes (Fig. 6b). In contrast, all isozymes oriented either in cytosol or the nucleus, namely, ACLY, ACO1, IDH1, MDH1, ME1, and ACSS2, were mostly expressed in CST-cHCECs. This finding is the first that the organelle-selective subcellular localization of metabolic isozymes is regulated by the cell (differentiation) state of cHCECs (Figs. 6a, b), which are distinct in their CD44 expression.

Impaired mitochondrial pyruvate uptake and OXPHOS result in metabolic reprogramming toward aerobic Warburg glycolysis.[35] Malic enzymes are known to catalyze the oxidative decarboxylation of malate to generate pyruvate and either nicotinamide-adenine dinucleotide phosphate, reduced form (NADPH) or nicotinamide adenine dinucleotide reduced form (NADH).[36] By recycling malate into the common TCA cycle carbon source pyruvate, malic enzymes may have a regulatory role in matching the TCA flux to cellular demand for energy (consistent with the present observations in Fig. 6b).

Mitochondria can control the expression of nuclear genes through a signaling from mitochondria to the nucleus.[37] Through this epigenetic mechanism, cells integrate environmental stimuli to tune gene expression levels.[38] Mitochondrial function and energy metabolism are tightly linked to the fate and function of a cell.[38]

Acetyl-CoA is a central molecule in cell metabolism, signaling, and epigenetics.[39–41] In mitochondria, acetyl-CoA is generated from pyruvate by the pyruvate dehydrogenase complex.[42] ACLY plays an important role in regulating histone acetylation levels in diverse mammalian cell types.[39,43–46] In addition to ACLY, nuclear-cytosolic acetyl-CoA is produced from acetate by ACSS2.[47] Considering the organelle selective localizations of ACLY and ACSS2, expressed only in CST-cHCECs (Fig. 6a) with decreased mitochondrial OCR, nuclear-cytosolic acetyl-CoA, but not in mitochondria matrix, play an epigenetic regulatory role in the generation of CST cHCECs.

Table. Fuel Dependency Test and Associated Inhibitors

Metabolic Test	Treatment 1	Treatment 2
Glucose dependency	UK5099	Etomoxir + BPTES
Glutamine dependency	BPTES	Etomoxir + UK5099
Fatty acid dependency	Etomoxir	BPTES + UK5099

The Fuel Dependency (%) = (Baseline OCR – Target inhibitor OCR)/(Baseline OCR- All inhibitors OCR) * 100 (%). BPTES; Bis-2-(5-phenylacetamido-1.3.4-thiadiazol-2-yl) ethyl sulfide. UK5099 was the mitochondrial pyruvate carrier inhibitor. BPTES was the glutaminase inhibitor. Etomoxir was the carnitine palmitoyltransferase 1A inhibitor.

Acknowledgments

The authors thank Munetoyo Toda, Asako Uehara, and Kazuko Asada for technical assistance; Yoko Hamuro and Keiko Takada for secretarial assistance; and Mr. John Bush for his excellent review of the manuscript. The authors also thank Takahiro Ito, Masahiro Yamashita, Yasuyuki Fujita, Shunsuke Kon, Mark A Greiner, and Kenjiro Kami for their scientific encouragement.

Supported by the Highway Program for Realization of Regenerative Medicine and Projects for Technological Development from the Japan Agency for Medical Research and Development, AMED, and JSPS KAKENHI (Grant Number JP26293376).

Disclosure: **K. Numa,** None; **M. Ueno,** None; **T. Fujita,** None; **K. Ueda,** None; **N. Hiramoto,** None; **A. Mukai,** None; **Y. Tokuda,** None; **M. Nakano,** None; **C. Sotozono,** None; **S. Kinoshita,** None; **J. Hamuro,** None

References

1. Dawson DG, Ubels JL, Edelhauser HF. Cornea and sclera. In: Levin LA, Nilsson SFE, Ver Hoeve J, Wu SM , eds. *Adler's Physiology of the Eye*. 11th ed. Edinburgh: Elsevier; 2011:71–130.
2. Kinoshita S, Koizumi N, Ueno M, et al. Injection of cultured cells with a ROCK inhibitor for bullous keratopathy. *N Engl J Med*. 2018;378:995–1003.
3. Koizumi N, Sakamoto Y, Okumura N, et al. Cultivated corneal endothelial cell sheet transplantation in a primate model. *Invest Ophthalmol Vis Sci*. 2007;48:4519–4526.
4. Okumura N, Ueno M, Koizumi N, et al. Enhancement on primate corneal endothelial cell survival in vitro by a ROCK inhibitor. *Invest Ophthalmol Vis Sci*. 2009;50:3680–3687.
5. Okumura N, Koizumi N, Ueno M, et al. ROCK inhibitor converts corneal endothelial cells into a phenotype capable of regenerating in vivo endothelial tissue. *Am J Pathol*. 2012;181:268–277.
6. Hongo A, Okumura N, Nakahara M, et al. The effect of a p38 mitogen-activated protein kinase inhibitor on cellular senescence of cultivated human corneal endothelial cells. *Invest Ophthalmol Vis Sci*. 2017;58:3325–3334.
7. Hamuro J, Toda M, Asada K, et al. Cell homogeneity indispensable for regenerative medicine by cultured human corneal endothelial cells. *Invest Ophthalmol Vis Sci*. 2016;57:4749–4761.
8. Toda M, Ueno M, Hiraga A, et al. Production of homogeneous cultured human corneal endothelial cells indispensable for innovative cell therapy. *Invest Ophthalmol Vis Sci*. 2017;58:2011–2020.
9. Hamuro J, Numa K, Fujita T, et al. Metabolites interrogation in cell fate decision of cultured human corneal endothelial cells. *Invest Ophthalmol Vis Sci*. 2020;61:10.
10. Maurice DM. The location of the fluid pump in the cornea. *J Physiol*. 1972; 221:43–45.

11. Bonanno JA. Molecular mechanisms underlying the corneal endothelial pump. *Exp Eye Res*. 2012;95:2–7.
12. Srinivas SP. Dynamic regulation of barrier integrity of the corneal endothelium. *Optom Vis Sci*. 2010;87:E239–E254.
13. Whikehart DR. The inhibition of sodium, potassium-stimulated ATPase and corneal swelling: the role played by polyols. *J Am Optom Assoc*. 1995;66:331–333.
14. Laing RA, Chiba K, Tsubota K, et al. Metabolic and morphologic changes in the corneal endothelium. The effects of potassium cyanide, iodoacetamide, and ouabain. *Invest Ophthalmol Vis Sci*. 1992;33:3315–3324.
15. Greiner MA, Burckart KA, Wagoner MD, et al. Regional assessment of energy-producing metabolic activity in the endothelium of donor corneas. *Invest Ophthalmol Vis Sci*. 2015;56:2803–2810.
16. Herrera AS, Esparza MDCA, Ashraf GM, et al. Beyond mitochondria, what would be the energy source of the cell? *Cent Nerv Syst Agents Med Chem*. 2015;15:32–41.
17. Tatsuta T, Langer T. Quality control of mitochondria: protection against neurodegeneration and ageing. *EMBO J*. 2008;27:306–314.
18. Youle RJ, van der Bliek AM. Mitochondrial fission, fusion, and stress. *Science*. 2012;337:1062–1065.
19. Wilson DF. Oxidative phosphorylation: regulation and role in cellular and tissue metabolism. *J Physiol*. 2017;595:7023–7038.
20. Hamuro J, Ueno M, Asada K, et al. Metabolic plasticity in cell state homeostasis and differentiation of cultured human corneal endothelial cells. *Invest Ophthalmol Vis Sci*. 2016;7:4452–4463.
21. Abe Y, Sakairi T, Kajiyama H, et al. Bioenergetic characterization of mouse podocytes. *Am J Physiol Cell Physiol*. 2010;299:C464–C476.
22. Stieger N, Worthmann K, Teng B, et al. Impact of high glucose and transforming growth factor-beta on bioenergetic profiles in podocytes. *Metabolism*. 2012;61:1073–1086.
23. Feeley KP, Westbrook DG, Bray AW, et al. An ex-vivo model for evaluating bioenergetics in aortic rings. *Redox Biol*. 2014;2:1003–1007.
24. Dunham-Snary KJ, Sandel MW, Westbrook DG, et al. A method for assessing mitochondrial bioenergetics in whole white adipose tissues. *Redox Biol*. 2014;2:656–660.
25. Winer LSP, Wu M. Rapid analysis of glycolytic and oxidative substrate flux of cancer cells in a microplate. *PLoS One*. 2014;9:e109916.
26. Benjamin T, Aldrich BT, Schlotzer-Schrehardt U, et al. Mitochondrial and morphologic alterations in native human corneal endothelial cells associated with diabetes mellitus. *Invest Ophthalmol Vis Sci*. 2017;58:2130–2138.
27. Hamuro J, Deguchi H, Fujita T, et al. Polarized expression of ion channels and solute carrier family transporters on heterogeneous cultured human corneal endothelial cells. *Invest Ophthalmol Vis Sci*. 2020;61:47.
28. Schneider CA, Rasband WS, Eliceiri KW. NIH Image to ImageJ: 25 years of image analysis. *Nat Methods*. 2012;9:671–675.
29. Kanda Y. Investigation of the freely-available easy-to-use software "EZR" (Easy R) for medical statistics. *Bone Marrow Transplant*. 2013:48,452–458.
30. Ueno M, Asada K, Toda M, et al. Gene signature-based development of ELISA assays for reproducible qualification of cultured human corneal endothelial cells. *Invest Ophthalmol Vis Sci*. 2016;57:4295–4305.
31. Zhang W, Li D, Diego G, et al. Glutaminolysis is essential for energy production and ion transport in human corneal endothelium. *EBioMedicine*. 2017;16:292–301.
32. Martinez-Reyes I, Chandel NS. Waste not, want not: lactate oxidation fuels the TCA cycle. *Cell Metab*. 2017;26:803–804.
33. Jin L, Alesi GN, Kang S. Glutaminolysis as a target for cancer therapy. *Oncogene*. 2016;35:3619–3625.
34. Wang Y, Dong C, Zhou BP. Metabolic reprogram associated with epithelial-mesenchymal transition in tumor progression and metastasis. *Genes Dis*. 2020;7:172–184.
35. Lee SM, Dho SH, Sung-Kyu J, et al. Cytosolic malate dehydrogenase regulates senescence in human fibroblasts. *Biogerontology*. 2012;13:525–536.
36. Jiang P, Du W, Mancuso A, et al. Reciprocal regulation of p53 and malic enzymes modulates metabolism and senescence. *Nature*. 2013;493:689–693.
37. Matilainen O, Quirós PM, Auwerx J. Mitochondria and epigenetics—crosstalk in homeostasis and stress. *Trends Cell Biol*. 2017;27:453–463.
38. Folmes C, Ma H, Mitalipov S, et al. Mitochondria in pluripotent stem cells: stemness regulators and disease targets. *Curr Opinion Genet Dev*. 2016;38:1–7.
39. Zhou SL, Li MZ, Li QH, et al. Differential expression analysis of porcine *MDH1*, *MDH2* and *ME1* genes in adipose tissues. *Genet Mol Res*. 2012;11:1254–1259.
40. Carrer A, Wellen KE. Metabolism and epigenetics: a link cancer cells exploit. *Curr Opin Biotechnol*. 2015;34:23–29.
41. Pietrocola F, Galluzzi L, Bravo-San Pedro JM, et al. Acetyl coenzyme A: a central metabolite and second messenger. *Cell Metab*. 2015;21:805–821.
42. de Boer VCJ, Houten SM. A mitochondrial expatriate: nuclear pyruvate dehydrogenase. *Cell*. 2014;158:9–10.
43. Covarrubias AJ, Aksoylar HI, Yu J, et al. Akt-mTORC1 signaling regulates Acly to integrate metabolic input to control of macrophage activation. *eLife*. 2016;5:e11612.
44. Donohoe DR, Collins LB, Wali A, et al. The Warburg effect dictates the mechanism of butyrate-mediated histone acetylation and cell proliferation. *Mol Cell*. 2012;48:612–626.
45. Lee JV, Carrer A, Shah S, et al. Akt-dependent metabolic reprogramming regulates tumor cell histone acetylation. *Cell Metab*. 2014;20:306–319.
46. Wellen KE, Hatzivassiliou G, Sachdeva UM, et al. ATP-citrate lyase links cellular metabolism to histone acetylation. *Science*. 2009;324:1076–1080.
47. Sutendra G, Kinnaird A, Dromparis P, et al. A nuclear pyruvate dehydrogenase complex is important for the generation of acetyl-CoA and histone acetylation. *Cell*. 2014;158:84–97.

Investigative Ophthalmology & Visual Science